Semiconductor Science and Technology

PAPER

Chlorine-based dry etching of β-Ga_2O_3

To cite this article: Jack E Hogan *et al* 2016 *Semicond. Sci. Technol.* **31** 065006

IOP Publishing Semiconductor Science and Technology
Semicond. Sci. Technol. **31** (2016) 065006 (6pp) doi:10.1088/0268-1242/31/6/065006

Chlorine-based dry etching of β-Ga_2O_3

Jack E Hogan, Stephen W Kaun, Elaheh Ahmadi, Yuichi Oshima and James S Speck

Materials Department, University of California, Santa Barbara, CA 93106, USA

E-mail: elaheh@ece.ucsb.edu (Elaheh Ahmadi)

Received 15 December 2015, revised 8 March 2016
Accepted for publication 17 March 2016
Published 14 April 2016

Abstract

Reactive ion etching (RIE) and inductively coupled plasma (ICP) etching techniques were used to determine the optimal dry etch conditions for β-Ga_2O_3. RF power and chamber pressure were examined to study their effects on etch rate and surface roughness for three crystallographic planes, i.e., (100); (010); and $(\bar{2}01)$ by RIE. BCl_3 etch rate calibrations were performed on all β-Ga_2O_3 planes studied, in comparison to Cl_2. RIE yielded moderate etch rates (<20 nm min^{-1}), and surface roughness showed no clear trend with RF power. Moreover, the effect of bias power, plasma power, and the choice of etchant were studied using ICP. The etches performed by ICP were shown to be superior to RIE in both etch rate and surface roughness, due to the much higher plasma densities and uniformities possible with plasma powers beyond those realized in RIE. The maximum etch rate of 43.0 nm min^{-1} was achieved using BCl_3 in ICP. SF_6/BCl_3 mixtures, which yield high GaN etch rates, were also studied. However, in contrast to GaN etching, SF_6/BCl_3 was found to be far less effective than pure BCl_3 in etching β-Ga_2O_3.

Keywords: β-Ga_2O_3, chlorine-based etch, dry etch, ICP, RIE

(Some figures may appear in colour only in the online journal)

Introduction

In recent years β-Ga_2O_3 has garnered attention as an exciting candidate for the active layer of future semiconducting devices. This is due in part to its wide bandgap of 4.8 eV, placing it well into the UV spectrum. As such, β-Ga_2O_3 is currently being developed for optical devices, such as ultraviolet detectors [1], and as a transparent epitaxial layer on GaN-based light-emitting diodes and lasers [2]. Additionally, β-Ga_2O_3 has recently been used for the fabrication of p-channel nanowire field effect transistors [3] and as the semiconducting material in traditional metal-oxide–semiconductor FETs [4]. An especially promising use of β-Ga_2O_3 is in vertical electron devices for high-power switching [5]. This is due to the previously mentioned remarkably wide bandgap as well as a high estimated breakdown field of 8 MV cm^{-1} [5]. The Baliga figure of merit—a central metric in power FETs comparing the conduction power losses between different materials [6]—places β-Ga_2O_3 above both SiC and GaN. Another advantage of β-Ga_2O_3 is the availability of inexpensive single-crystal substrates due to growth by relatively low-cost melt-based growth techniques. This is highly advantageous in the fabrication of vertical devices where mass production requires large, single crystal wafers. This has been accomplished through floating-zone [7, 8], Czocharalski [9] and edge-defined film fed growth [10].

Still, significant research is required before β-Ga_2O_3 devices will be practical for large-scale production. Previous studies have shown β-Ga_2O_3 can be n-type doped with Si or Sn, and Ohmic contacts can be formed with a Ti/Au stack annealed in N_2. There are however, few studies of suitable etching conditions for β-Ga_2O_3 [11, 12]. These conditions determine the etch rate, roughness, and anisotropy of the exposed surface—each being essential parameters of any device fabrication process. In contrast, GaN has extensively developed etch technologies. Despite the different crystal structure and anion for GaN and β-Ga_2O_3, $GaCl_3$ is a likely volatile product for both materials under chlorine-based etches. The preferred etch for GaN uses chlorine in the form of BCl_3 and Cl_2. In this mixture, the Cl_2 is the primary etchant, while the BCl_3 removes the native oxide and improves sidewall passivation [13]. Due to the chemical similarity between GaN and β-Ga_2O_3, GaN etch conditions were chosen as the starting point for the exploration of β-Ga_2O_3 etch parameters.

Two dry etch techniques are typically employed in compound semiconductor device fabrication—reactive ion

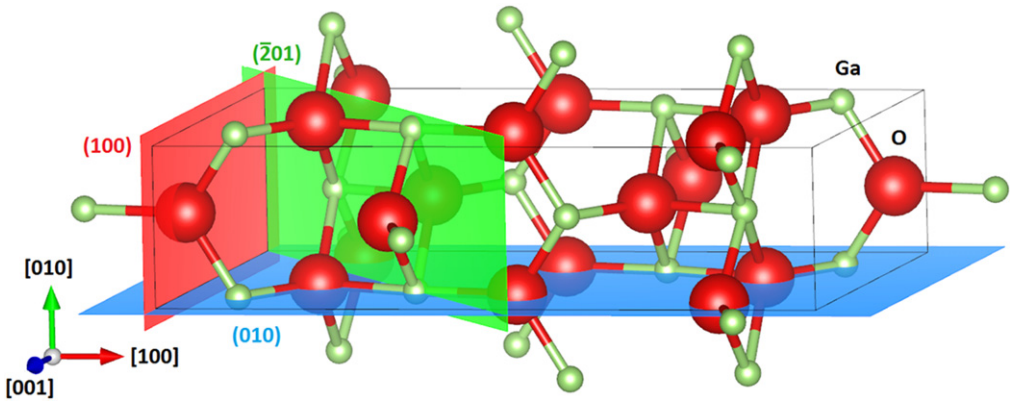

Figure 1. The β-Ga_2O_3 unit cell with the (100), (2̄01) and (010), crystallographic planes shown in red, blue, and green, respectively.

etching (RIE) and inductively coupled plasma (ICP) etching. Each technique operates under the principle of ionizing a gas and propelling the ions towards the substrate surface, but they differ in the manner by which the gas is ionized. In RIE, the sample is placed on an electrode that is driven at 13.56 MHz. As the etchant gas flows over, it is ignited by the potential difference (RF power), becoming a plasma consisting of positive ions, radicals, and electrons. The high mobility of the electrons compared to the ion and radical components causes the electrode to acquire a negative charge. The positive ions in turn are accelerated towards the substrate and react with the surface atoms [14]. In contrast, in ICP etching the plasma is generated using a magnetic field by applying RF power to a coil (plasma power). Once the plasma is ignited, the ions are accelerated towards the substrate in the same manner as RIE. The advantage of ICP is that very high ion densities can be achieved leading to higher etch rates than RIE. Additionally, because the plasma is generated by a magnetic field in ICP etching, a lower bias is needed to propel the ions toward the sample, which reduces surface damage [15]. In either technique, the etch rate is a result of this combined action of surface chemical reactions and physical ion bombardment.

β-Ga_2O_3 exists in a monoclinic crystal lattice with lattice parameters of $a = 1.22$ nm, $b = 0.304$ nm, $c = 0.580$ nm, $\alpha = \gamma = 90°$, and $\beta = 103.8°$. The unit cell shown in figure 1 has two gallium sites: one in tetrahedral geometry; the other octahedral—while the oxygen anions form a distorted cubic close packing arrangement [16]. The (100) plane is the strong cleavage plane and was initially the subject of the majority of growth studies. However, due to relatively weak surface bonds growth on this plane is difficult. The low adhesion energy on the (100) terraces promotes the formation of volatile gallium suboxides which compete with growth [17]. As such, focus has since shifted to the the (010) and (2̄01) planes. The (010) plane is a non-cleaveage plane made up of gallium atoms in both tetrahedrally coordinated and octahedrally coordinated sites, as well as oxygen atoms. The (2̄01) plane consists exclusively of octahedrally bonded gallium atoms.

In this paper, we determine the etch rate and etch morphology for three important crystal planes of β-Ga_2O_3 using RIE and ICP etching. We demonstrate that ICP etching with BCl_3 gas results in smooth morphologies and high rates for the (010) plane.

Experiment

This study focused on different β-Ga_2O_3 etch conditions for the primary growth planes—(100), (010), and (2̄01). Specifically, the effects of power, chamber pressure, and etchant gas were examined using both ICP (Panasonic E6261) and RIE (Plasma-Therm SLR-770) apparatuses in the UCSB nanofabrication facility.

Free-standing UID and Sn-doped β-Ga_2O_3 substrates were diced into $\sim 5 \times 5\,mm^2$ pieces for etch tests. Each sample was cleaned using acetone, isopropanol, and deionized water. Timed etches were first performed with a Kapton tape mask and subsequently verified using a photoresist mask (Shipley SPR 220 photoresist). In the RIE etch studies, power, chamber pressure, and etchant gas flow rates were investigated. The control values for each variable were chosen with respect to standard GaN etch conditions, for which there is readily available data. The etch rates were tested at RF powers of 50, 100, 200, and 250 W. Chamber pressures were tested at 5, 10, and 20 mTorr. Finally the etchant gas flow rates for Cl_2/BCl_3 were tested at 20/0, 15/5, 10/10, 5/15, and 0/20 sccm. ICP was used to test a variety of etchant gases and to study the effect of plasma and bias power. In addition to BCl_3, CF_4/O_2, and SF_6, were also tested on gallium oxide. The etching time for each experiment was 10–30 min.

After removal from the etch chamber, samples were again cleaned using the aforementioned solvents. Etched feature heights were determined using a Dektak stylus profiler. Roughness measurements were performed using atomic force microscopy (AFM).

Results

Reactive ion etching

To determine the viability of different etch conditions, the surface roughness and etch rate achieved were assessed for

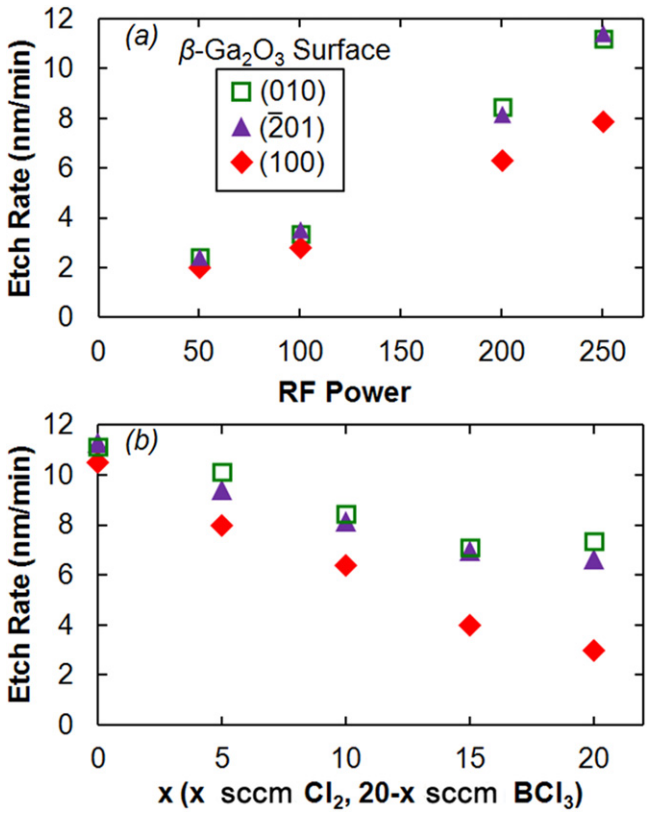

Figure 2. (a) RIE etch rate for differing RF powers with a constant Cl_2:BCl_3 ratio of 10:10 sccm. (b) RIE etch rate for differing Cl_2:BCl_3 ratios with an RF power of 200 W. In each case the chamber pressure is 10 mTorr.

each case. In changing the etch conditions, RF power, chamber pressure, and etchant gas flow rates (Cl_2/BCl_3 sccm) were all varied on β-Ga_2O_3 (100), (010), and ($\bar{2}01$) surfaces using RIE.

Our initial work focused on the RF power supplied to the Cl_2/BCl_3 gas mixture, where increases in power significantly impacted the plasma activation, yielding an approximately linear relationship between RF power and etch rate. As shown in figure 2(a) an increase of RF power from 50 to 250 W corresponded to an etch rate increase from 2.0 to 11.5 nm min^{-1} for the (010) plane. At RF powers greater than 250 W, the reflected power of the system markedly increased; thus, 250 W was the highest RF power tested. With 200 W RF power adding no risk of plasma instability and providing etch rates greater than 5 nm min^{-1} for each studied crystal plane, this RF power was used in the remainder of the Cl_2/BCl_3 flow rate study.

The etchant gas ratio had a significant effect on the etch rate. It was found that a pure BCl_3 etch was much more effective than a pure Cl_2 etch, and a mixture of the two resulted in a etch rate roughly related to the weighted average of each etchant as shown in (figure 2(b)). This linear relationship when using mixtures of BCl_3 and Cl_2 may be indicative of minimal interaction between the etch species. Interestingly BCl_3 etches at similar rates for all three planes while Cl_2 etched the (010) and ($\bar{2}01$) planes at a higher rate than the (100) plane. Another difference between the two etchants is their selectivity to the photoresist. Cl_2 quickly removed the photo resist at 200 W while the BCl_3 showed no ability to etch it. This supports the idea that each etching processes contain different active species present in the plasma, though $GaCl_3$ and O_2 are nonetheless expected as an etch products in either case.

Increasing the chamber pressure from 5 to 20 mTorr increased the etch rate on the (100) and (010) planes from 4.2 to 8.1 nm min^{-1} and 7.1 to 10.5 nm min^{-1}, respectively. As expected, this effect is linear, since higher etchant ion densities result in a greater frequency of ion-substrate collisions.

The (010) and ($\bar{2}01$) planes were consistently etched at a higher rate than the (100) surface. The (100) plane has strong lateral bonds and a relatively weak bonds normal to the plane direction resulting in a strong cleavage plane that is difficult to etch. We speculate that the surface is made entirely of oxygen atoms (see figure 1), and the electronegative oxygen provides a surface resistance to etching involving Cl^- or BCl^- anions. The electrostatic repulsion of the reactive anions with the surface oxygen anions decreases the ability to etch the surface and the recessed gallium cations are, in effect, inaccessible and protected, leading to a decreased etch rate. Unlike the (100) plane, the non-cleavage (010) plane is composed of gallium atoms, and the ($\bar{2}01$) plane is a weak cleavage plane composed of both gallium and oxygen atoms. While the exact etching mechanism is not entirely understood, the availability of surface gallium atoms on the (010) and ($\bar{2}01$) planes provides insight that suggests a favorable reaction between gallium and the impinging activated chlorine. This is also justified through the noted etch product of $GaCl_3$. The accessibility of these reactant gallium cations, therefore, can explain the observed face-dependent trend in etch rates. However, this does not consider possible surface reconstructions or other factors influencing the lattice, such as differing bond angles and energies. The other possibility is the difference in the density of the dangling bonds on different planes. Based on the assumption that dangling bonds are vulnerable to the etching gas. Therefore, higher density of dangling bonds on (010) and ($\bar{2}01$) planes could result in higher etch rates.

ICP etching

ICP was used to investigate the performance of a wider variety of etchant gases; the effect of plasma (ICP) and forward (capacitively coupled plasma) powers were also analyzed. Specifically, the etchant gases used were BCl_3, a mixture of BCl_3/SF_6, and CF_4/O_2.

The combination of BCl_3/SF_6 has previously been shown to increase the etch rate and selectivity of GaN [18]. Addition of other gases is expected to reduce the probability of boron–chlorine recombination, leading to higher active chlorine, which is line with the proposed mechanism [19]. Etchant gas flow ratios of 15:5 sccm and 5:15 sccm BCl_3:SF_6 were compared to BCl_3 alone. Chamber conditions used plasma and bias powers of 200 and 30 W, respectively. As shown in table 1, the etch rates for β-Ga_2O_3 involved a significant reduction when using either gas mixture as opposed

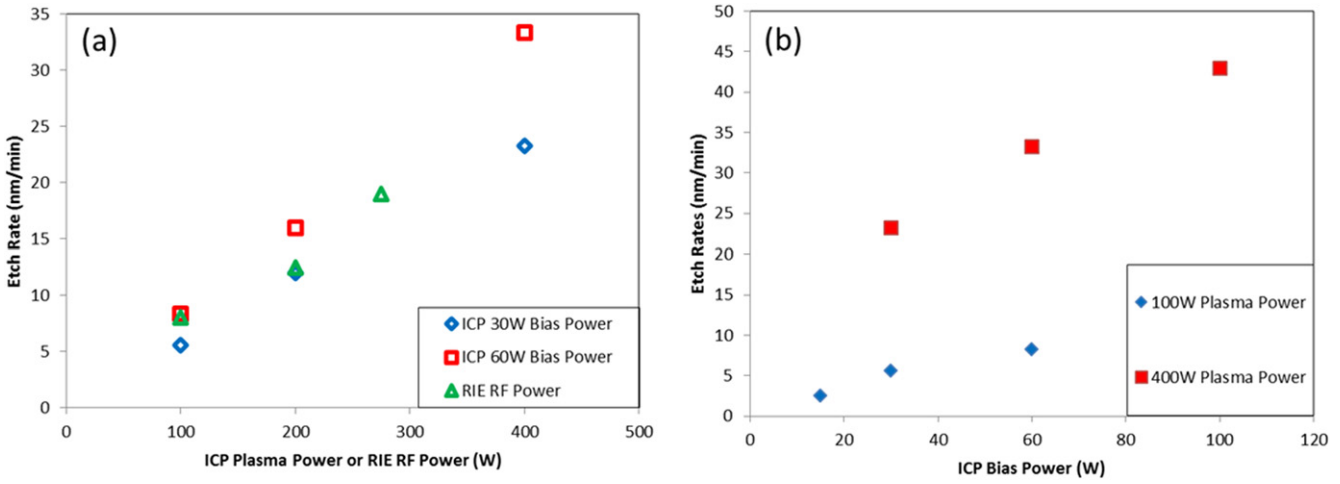

Figure 3. (a) Etch rate as a function of ICP plasma power and RIE RF power, (b) etch rate as a function of ICP bias power. In each case chamber conditions were 15 mTorr and 20 sccm BCl_3.

to BCl_3 alone; this is the opposite effect to GaN. The BCl_3 rich gas mixture had a higher etch rate of 3.1 nm min^{-1}, compared to 1.5 nm min^{-1} for the CF_4/O_2 mixture, but both can be considered ineffective compared to the etch rate of 12 nm min^{-1} for BCl_3 at the same conditions. This marked decrease in etch rate can likely be attributed to the formation of GaF_3 which acts as an etch inhibitor because of its low volatility [18].

Using BCl_3, etch studies were conducted to alter plasma and bias power. These are shown in figure 3. These results, although limited in number, suggest etch rate and plasma power are linearly related. Considering plasma density is dependent on plasma power it is likely this relationship is linear as well. Additionally the etch mechanism seems to be related primarily to the incident ion flux to the surface, rather than any surface diffusion/reactions or desorption rates.

Table 1. ICP Etch rates for various etchant gases on (010). Chamber conditions are 15 mTorr with source/bias power 200/30 W.

Etchant gas	BCl_3 20 sccm	CF_4/O_2 20/2 sccm	BCl_3/SF_6 15/5 sccm	BCl_3/O_2 5/15 sccm
Etch rate (nm min^{-1})	12.0	1.5	3.1	2.3

Surface roughness

Surface morphologies of samples etched under various conditions are shown in figure 4. ICP yielded lower surface roughness than RIE for equivalent etch depths. This is likely due to the different mechanisms for ionization of the etchant gas between the two systems. In RIE a large forward bias is required to ionize the etchant gases and accelerate them towards the surface. At higher forward biases ions impact the surface with greater kinetic energy which may lead to physical sputtering in addition to chemical etching. Furthermore, uneven etch profiles were observed on RIE-etched samples for all RF powers, possibly the result of incomplete removal of etch products acting as micro-masks. This may be explained by non-uniformity in the plasma as the RF power in RIE appears to be too low to homogeneously ignite the plasma. This deleterious effect appears to be absent in ICP, since the plasma is generated through a magnetic field prior to applying forward plasma. The resulting effect is two-fold, much higher plasma densities are possible in ICP in comparison to RIE and, therefore, much lower forward bias is required to accomplish similar etch rates. In figure 4, comparing the 100 W bias power cases, there appear to be fewer inhomogeneous surface features on the ICP sample, though as indicated the etch rate is higher. This can be rationalized by the higher plasma density promoting isotropic chemical etching that partial negate the formation of unwanted features caused by physical bombardment; this combined physico-chemical action is the reason for both higher etch rates and a more uniform surface.

Mesa structure

We investigated the steepness of mesa structure of a sample formed by ICP etching using a condition under which both good surface morphology and high etch rate was achieved. BCl_3 with a flow rate of 20 sccm was used as the etchant gas for this sample. The etch was performed for half an hour using source and bias powers of 200 and 30 W, respectively. figure 4 shows a scanning electron microscope (SEM) image of the sample. It was found that a relatively, steep wall was achieved using the abovementioned etch conditions.

Summary

The effects of etchant gas, chamber pressure, and power for both RIE an ICP etching processes has been investigated on the (100), (010), and $(\bar{2}01)$ planes of β-Ga_2O_3 to determine the optimal conditions for both etch rate and surface

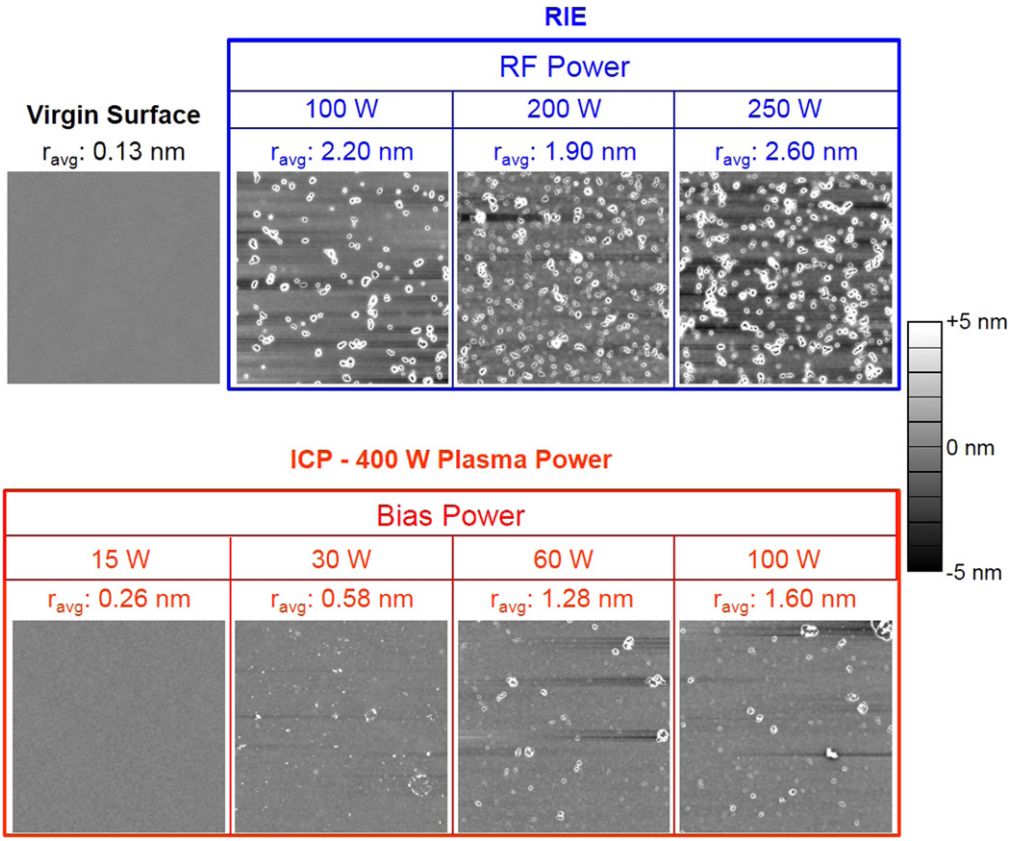

Figure 4. Roughness data using AFM taken for both RIE and ICP etches at differing powers on the (010) plane. Roughness is computed as the average of three 5 × 5 μm^2 scans.

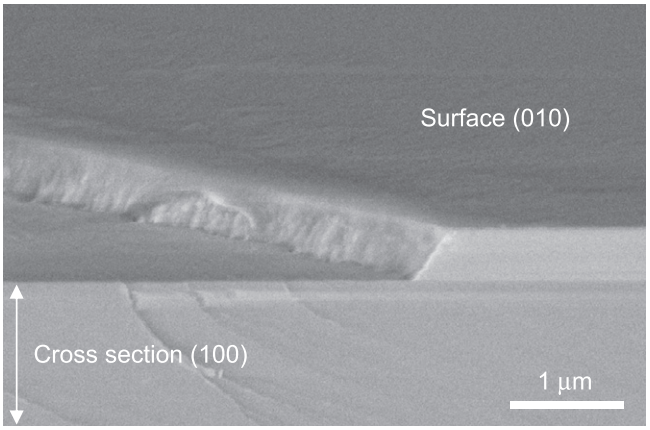

Figure 5. SEM image (bird's-eye view) of an sample etched by ICP with 20 sccm BCl_3 for half an hour using plasma and bias powers of 200 W and 30 W, respectively.

roughness. The RIE and ICP etching conditions are summarized in tables 2 and 3, respectively. The two planes that are most promising for power electron devices—(010) and (201)—performed similarly across all tests, while the (100) plane showed lower etch rates. Of the etchant gases tested (BCl_3, Cl_2, CF_4, and SF_6), BCl_3 produced the highest etch rate. In contrast to previous studies on GaN, the addition of SF_6 to BCl_3 to the etch gas did not increase the etch rate, but rather decreased it drastically. Increasing RF power in RIE increased the etch rate without showing a clear pattern in surface roughness. The maximum RF power of 250 W produced an etch rate of 19 nm min^{-1} on (010). RIE was outperformed by ICP likely due to higher plasma density. ICP conditions of 400 W/100 W plasma/bias power (highest tested) using BCl_3 had an etch rate of 33 nm min^{-1} with lower surface roughness than any RIE samples. The results of this study indicate that ICP is preferred over RIE to etch β-Ga_2O_3,

Table 2. A summary of RIE etch conditions studied in this work.

RIE	Power study		Gas ratio study	Pressure study
RF power (W)	50, 100, 200, 250	100, 200, 250	200	
Cl_2/BCl_3 (sccm)	10/10	0/20	20/0, 15/5, 10/10, 5/15, 0/20	10/10
Pressure (mTorr)	10	15	10	5,10,20
Plane	a, b, $(\bar{2}01)$	b	a, b, $(\bar{2}01)$	a,b
Results shown in	Figure 1(a)	Figure 3(a)	Figure 1(b)	text

Table 3. A summary of ICP etch conditions studied in this work.

ICP	Plasma power study		Bias power study		Gas ratio study	
Plasma power (W)	100, 200, 400		100	400	200	
Bias power (W)	30	60	15, 30, 60	15, 30, 60, 100	30	
BCl_3/CF_6 (sccm)			20/0		15/5, 5/15, 20/0	—
CF_4/O_2 (sccm)			—		—	20/2
Pressure (mTorr)				15		
Plane				b		
Results shown in	Figures 3(a), 4		Figure 3(b)	Figures 3(b), 5	table 1	

and using BCl_3 as the etchant is advised. Acceptable surface roughness was shown below 400 W/100 W plasma/bias power.

Acknowledgment

This work was supported by the Air Force Office of Scientific Research (AFOSR, Program Manager Dr Ali Sayir) through grant number FA9550-14-1-0112. Additional support for JEH, SWK and JSS was provided by the MRSEC Program of the US National Science Foundation under Award No. DMR-1121053.

References

[1] Kokubun Y, Miura K, Endo F and Nakagomi S 2007 Sol–gel prepared β-Ga_2O_3 thin films for ultraviolet photodetectors *Appl. Phys. Lett.* **90** 1–4

[2] Víllora E G, Arjoca S, Shimamura K, Inomata D and Aoki K 2014 *Proc. SPIE* **8987** 89871U

[3] Chang P C, Fan Z, Tseng W Y, Rajagopal A and Lu J G 2005 β-Ga_2O_3 nanowires: synthesis, characterization, and p-channel field-effect transistor *Appl. Phys. Lett.* **87** 1–3

[4] Matsuzaki K, Yanagi H, Kamiya T, Hiramatsu H, Nomura K, Hirano M and Hosono H 2006 Field-induced current modulation in epitaxial film of deep-ultraviolet transparent oxide semiconductor Ga_2O_3 *Appl. Phys. Lett.* **88** 88–91

[5] Higashiwaki M, Sasaki K, Kuramata A, Masui T and Yamakoshi S 2012 Gallium oxide (Ga_2O_3) metal–semiconductor field-effect transistors on single-crystal β-Ga_2O_3 (010) substrates *Appl. Phys. Lett.* **100** 1–4

[6] Baliga B J 1989 Power semiconductor device figure of merit for high-frequencyapplications *IEEE Electron Device Lett.* **10** 455–7

[7] Villora E G, Shimamura K, Yoshikawa Y, Aoki K and Ichinose N 2004 Large-size β-Ga_2O_3 single crystals and wafers *J. Cryst. Growth* **270** 420–6

[8] Tomm Y, Ko J M, Yoshikawa A and Fukuda T 2001 Floating zone growth of β-Ga_2O_3: a new window material for optoelectronic device applications *Sol. Energy Mater. Sol. Cells* **66** 369–74

[9] Tomm Y, Reiche P, Klimm D and Fukuda T 2000 Czochralski grown Ga_2O_3 crystals *J. Cryst. Growth* **220** 510–4

[10] Aida H, Nishiguchi K, Takeda H, Aota N, Sunakawa K and Yaguchi Y 2008 Growth of β-Ga_2O_3 single crystals by the edge-defined, film fed growth method *Japan. J. Appl. Phys.* **47** 8506–9

[11] Higashiwaki M, Sasaki K, Kuramata A, Masui T and Yamakoshi S 2012 Gallium oxide (Ga_2O_3) metal–semiconductor field-effect transistors on single-crystal β-Ga_2O_3 (010) substrates *Appl. Phys. Lett.* **100** 013504

[12] Oshima T, Okuno T, Arai N, Kobayashi Y and Fujita S 2009 Wet etching of β-Ga_2O_3 substrates *Japan. J. Appl. Phys.* **48** 040208

[13] Rawal D S, Malik H K, Agarwal V R, Kapoor A K, Sehgal B K and Muralidharan R 2012 BCl_3Cl_2 based inductively coupled plasma etching of GaN/AlGaN using photoresist mask *IEEE Trans. Plasma Sci.* **40** 2211–20

[14] Oehrlein G S 1986 Reactive-ion etching *Phys. Today* **39** 26

[15] Smith S A, Wolden C A, Bremser M D, Hanser A D, Davis R F and Lampert W V 1998 Selective and non-selective etching of GaN, AlGaN, and AlN using aninductively coupled plasma *Compound Semiconductors 1997, Proc. IEEE 24th Int. Symp. on Compound Semiconductors* vol 3631 pp 19–22

[16] Åhman J, Svensson G and Albertsson J 1996 A reinvestigation of β-gallium oxide *Acta Crystallogr.* C **52** 1336–8

[17] Sasaki K, Higashiwaki M, Kuramata A, Masui T and Yamakoshi S 2013 MBE grown Ga_2O_3 and its power device applications *J. Cryst. Growth* **378** 591–5

[18] Buttari D, Chini A, Chakraborty A, Mccarthy L, Xing H, Palacios T, Shen L, Keller S and Mishra U K 2004 Selective dry etching of GaN over AlGaN in BCL_3/SF_6 mixtures *Int. J. High Speed Electron. Syst.* **14** 756–61

[19] Oh C S, Kim T H, Lim K Y and Yang J W 2003 GaN etch enhancement in inductively coupled BCl3 plasma with the addition of N_2 and SF_6 gas *Semicond. Sci. Technol.* **19** 172–5